Measurement of Diffusivity of a Liquid Diamine in Solid Epoxies Using Attenuated Total Reflectance Infrared Spectroscopy (FTIR-ATR)

T. P. SKOURLIS and R. L. MCCULLOUGH*

Department of Chemical Engineering, Center for Composite Materials, University of Delaware, Newark, Delaware 19716

SYNOPSIS

A number of studies on thermosetting polymeric composite materials have indicated the existence of a three dimensional region of the matrix in the vicinity of the fiber, which exhibits distinct properties. A key factor in the interphase formation of epoxy–diamine mixtures is the diffusivity of the diamine relative to the epoxy prepolymer. A technique for measuring diffusion coefficients of a liquid through solid polymeric thin layers is described. Infrared attenuated total reflectance (ATR) spectroscopy is used to analyze diffusion couples with infrared distinguishable bands. A cylindrical germanium crystal, coated with the polymeric layer of interest, is immersed in a boat cell filled with the diffusant, and infrared spectra of the system are taken in real time. By those means, only the region close to the solid surface is scanned without interferences from the bulk. The temperature dependence of diffusivity can also be evaluated by the use of a heated cell. Diffusivities that are evaluated in this way can be used to predict stoichiometric gradients during the curing reaction of the system and, therefore, the structure and property gradients of the material around the fiber. © 1994 John Wiley & Sons, Inc.

INTRODUCTION

Polymeric Composite materials' properties can be influenced by the existence of a perturbed, three dimensional region of the matrix in the vicinity of the fiber. Studies[1-3] have shown that the interphase might be less rigid than the bulk, due to the modification of the curing kinetics by the fiber surface. Palmese and McCullough[2] reported the results of a thermodynamic model that predicts interfacial stoichiometric gradients, developed during curing, of a carbon fiber/epoxy matrix system. According to this model, a matrix zone of lower glass transition temperature and modulus than the bulk matrix is generated as a consequence of concentration gradients. These results were verified by single fiber elevated temperature experiments.[3]

Sizings have been traditionally applied on fiber surfaces for commercial applications. The effect of silane coupling agents on glass fiber surfaces has been extensively characterized. Carbon fibers, on the other hand, are usually supplied with an epoxy-based coating on their surface, which is expected to affect interfacial and composite properties. Sizings can be mixtures of different additives that are applied on fibers by solution or emulsion coating. Their main purpose is to enhance handling and processing of the fibers. The effect of those sizings is not completely understood as far as composite properties are concerned. It is likely that the interphase properties of the composite are dominated by the diffusion and reaction processes taking place inside the coating region during the curing of the entire system.

The most widely used methods for the evaluation of diffusivities of small molecules inside solid polymeric films are gravimetric. Plots of mass gained vs. $t^{1/2}$, when Fickian diffusion is followed, can produce diffusivities either using initial slope or half sorption times. The time to reach equilibrium can be a critical factor for these experiments, since low diffusivity ($< 10^{-11}$ cm^2/sec) evaluation requires thin diffusing path lengths (and thin samples) for reasonable experimental times.

* To whom correspondence should be addressed.

Journal of Applied Polymer Science, Vol. 52, 1241–1248 (1994)
 CCC 0021-8995/94/091241-08

In order to achieve low path lengths, in cases such as polymer melt interdiffusion, where gravimetric techniques are difficult to use, spectroscopic methods have been applied. These include forced Raleigh scattering, spin echo NMR, and infrared microdensimetry. An infrared ATR technique has been developed for diffusivity measurements. The applications of this method include diffusion of $CaCO_3$ out of latex paint films,[4,5] water diffusion in polymer or asphalt–metal interfaces,[6] polymer melt mutual diffusion,[7] and water in polyacrylonitrile diffusion.[8]

Fourier transform infrared-attenuated total reflection spectroscopy (FTIR-ATR) is an extremely sensitive method for studying molecular changes at the surface and the interface. A unique aspect of internal reflection spectroscopy is the use of an optically dense medium, internal reflection element (IRE), as an optical guide to obtain an infrared spectrum. The IR radiation, above the critical angle, is totally reflected at the IRE/air interface. At the point of reflection, the radiation goes out of the element and forms an evanescent wave, which is the interference wave of the incident and reflected waves.[9]

The amplitude of the evanescent wave decays exponentially from the surface, which means that the largest contribution to the spectrum comes from the material within the penetration depth, d_p. The penetration depth is defined as the distance from the surface, over which the magnitude of the penetrating electric field diminishes by a factor of $1/e$, and is given by the following equation:

$$d_p = \frac{\lambda}{2\pi n_1\left[\sin^2\theta - \left(\frac{n_2}{n_1}\right)^2\right]^{1/2}} \qquad (1)$$

where λ is the wavelength in vacuum, θ is the angle of incidence, and n_1 and n_2 are the refractive indices of the internal reflection element and the material in contact with the IRE, respectively.[9]

When an infrared absorbing material is in contact with an internal reflection element, the evanescent wave interacts with the material and causes the attenuation of the total reflection of the propagating beam inside the IRE. Detection of the attenuated radiation leaving the element yields an IR spectrum of the sample. The absorbance is expressed by the following equation, which is the equivalent to Beer–Lambert's law for transmission:

$$A \approx \int_0^\infty a \exp\left(\frac{-2x}{d_p}\right) c(x) S \, dx \qquad (2)$$

where x is the distance from the surface, c is the concentration, a is the oscillator strength, and S is the cross sectional area.

In order to use the above principles for diffusivity measurements, diffusion couples are prepared by sandwiching layers of the two components on the surface of an internal reflection crystal. The diffusion process is therefore monitored in real time by measuring the absorbance of the characteristic band of one of the two components. Fitting the experimental data to the solution of the diffusion equation, as it is applied in this system, will yield diffusivity values.

The advantages of using an FTIR-ATR technique over other existing methods for diffusivity evaluation include the *in situ* measurement of concentrations along with the possibility of achieving small penetration depths (of the order of 0.1 μm). These characteristics allow for the minimization of the effects of the two species' interfacial interactions. In addition, the effect of the presence of a solid surface in the vicinity of the diffusion system can be investigated. Bulk phase homogeneous chemical reactions and interactions, such as hydrogen bonding between the two species, can be simultaneously monitored if the necessary bands are detectable and distinguishable. Finally, the method is not limited by the phase of the two components of the system, since the use of a suitable ATR fixture allows for the study of liquid–solid, as well as liquid–liquid, diffusion couples.

EXPERIMENTAL

Optical Property Evaluation

In order for the FTIR-ATR method to be used quantitatively, an accurate value for the penetration depth d_p is needed. According to eq. (1), d_p depends on the wavelength of interest, the properties of the crystal, which are supplied by the manufacturer, and the refractive index of the polymer. Since optical properties for polymers in the infrared region of the spectrum are scarce in the literature, it is necessary to measure them experimentally.

A simple way of measuring the optical constants of interest is by identifying the critical angle θ_c.[9] This parameter is defined as the minimum angle of incidence at which total internal reflection takes place, and is expressed by eq. (3):

$$\theta_c = \sin^{-1}\left(\frac{n_2}{n_1}\right) \qquad (3)$$

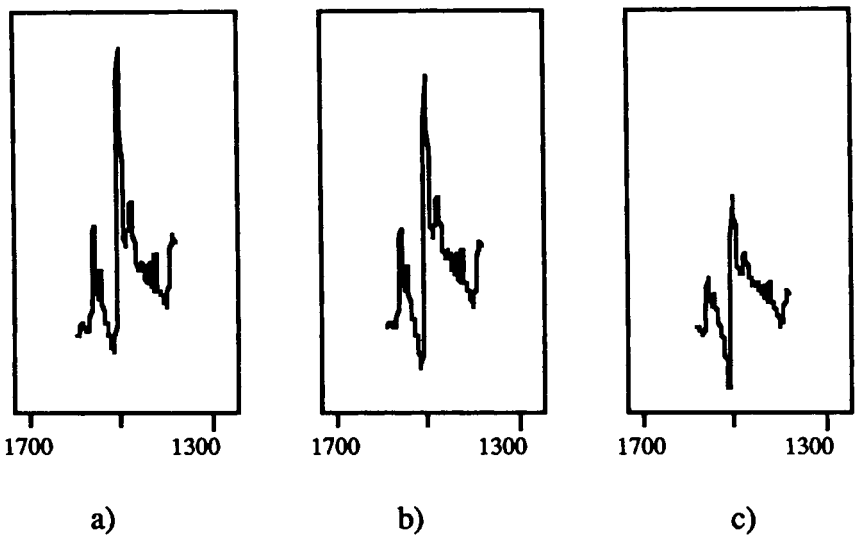

Figure 1 Epoxy spectrum variation with angle of incidence: (a) $\theta = 20°$, (b) $\theta = 18°$, (c) $\theta = 15°$. Transition from normal absorption to refractive index dispersion.

This method involves collecting variable angle internal reflection spectra for the polymer of interest in contact with a surface of a known refractive index. At the point of transition from normal absorption (where spectra are similar to transmission ones) to refractive index dispersion (where spectra look distorted), the critical angle is measured and n_2 is calculated using eq. (3).

A film of the solid epoxy polymer, diglycidyl ether of bisphenol-A (EPON 1001F, Shell Chemical Co.), was solution cast from a methylene chloride solution on the surface of a semispherical germanium crystal, which served as the IRE. This crystal was then mounted on a variable angle reflection accessory (Seagull, Harric Scientific Corporation). Single internal reflection through the crystal was conducted under a variety of angles of incidence. A characteristic peak of the epoxy (around 1506 cm^{-1}) was monitored and some spectra are shown in Figure 1.

The critical angle for epoxy EPON 1001F was determined to be 16 ± 1°. Using eq. (3) and the index of refraction for germanium equal to 4.0, the index of refraction for the epoxy was calculated to be 1.1 ± 0.1. This value holds only for wavenumbers close to 1500 cm^{-1}, since refractive indices have been known to depend strongly on wavelength.

It must be pointed out here that the method used to determine optical constants is not accurate, but is useful only for an order of magnitude analysis, since it is usually hard to determine the exact point of transition at the critical angle. However, the penetration depth is the only parameter, in terms of material properties, necessary for the application of the diffusivity evaluation FTIR-ATR method described here. In order to examine the sensitivity of our optical constants evaluation method, the penetration depth was plotted in Figure 2 vs. the critical angle. For this calculation, eqs. (1) and (3) were used. In addition, an angle of incidence of 60° and the index of refraction for germanium were also used according to the specifications of the IRE for most of the diffusivity experiments. It is evident from Figure 2 that the penetration depth is not sensitive to θ_c variations and, therefore, a penetration depth of 0.32 ± 0.05 μm is used in the following analysis.

FTIR–Cylindrical Internal Reflection Technique

The technique used for diffusivity evaluation was based on a cylindrical internal reflection accessory

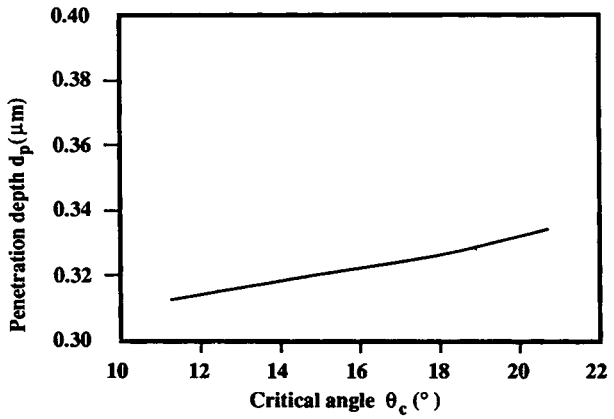

Figure 2 Penetration depth for the germanium crystal ($\theta = 60°$)/EPON 1001F system used in diffusivity experiments vs. θ_c range, over which some uncertainty over the transition point existed.

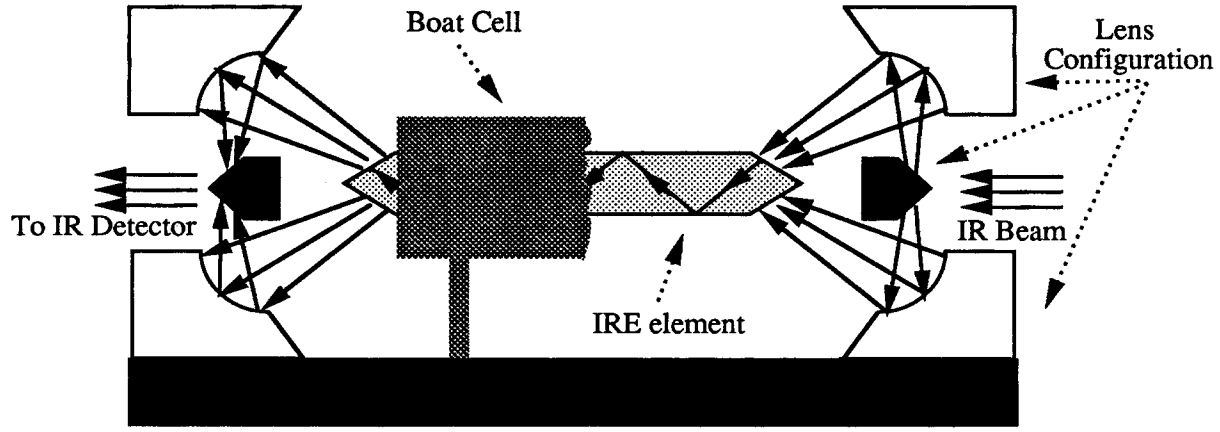

Figure 3 Cylindrical internal reflection accessory.

(Circle, Spectra Tech Inc.). This accessory consists of a $\frac{1}{8}$ in. diameter cylindrical germanium crystal with conical ends and an open boat cell for liquid samples. The open boat configuration can be covered by a high temperature cell, offering the possibility of high temperature studies. This type of accessory has been used mainly for aqueous solutions with detection limits as low as 0.1%. The accessory used is shown schematically in Figure 3.

The cylindrical crystal was coated with a film of EPON 1001F by solution coating from a methylene chloride solution (10% w/w concentration). Coating thicknesses were calculated gravimetrically, based on the density of the polymer film and the assumption of uniform thickness of the film. After coating, the cylinder was placed inside the open boat cell. Diffusion experiments started by filling the boat cell with the diffusant, which was a diamine, *bis*(*p*-amino cyclohexyl) methane (Amicure PACM-20, Air Products Inc.).

The boat cell assembly was mounted within an infrared spectrometer (Nicolet 20DXB). The chamber was purged with dry air during the experiments. The spectrometer was equipped with a triglycine sulfate (DTGS) detector. A resolution of 4 cm^{-1} was used and 32 scans per sampling were taken, leading to sampling times on the order of 30 sec. Before the initiation of the experiment, the spectrum of the environment of the chamber was taken, to be used as a background for all the spectra. All spectra were plotted in the absorbance (A) mode and quantitative analysis was performed using the peak height method for the bands of interest.

Spectra Identification

For the FTIR-ATR method to provide useful information on diffusion processes, distinguishable bands for the two components of the diffusion couple must be identified. Spectra for EPON 1001F and PACM

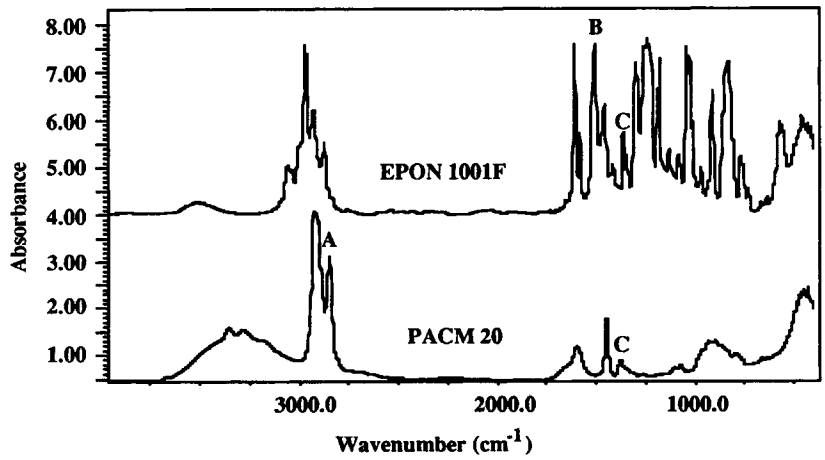

Figure 4 Spectra for diffusion couple: peak A is C—H stretch (cyclohexane ring), peak B is C—C stretch (aromatic), and peak C is C—H bending.

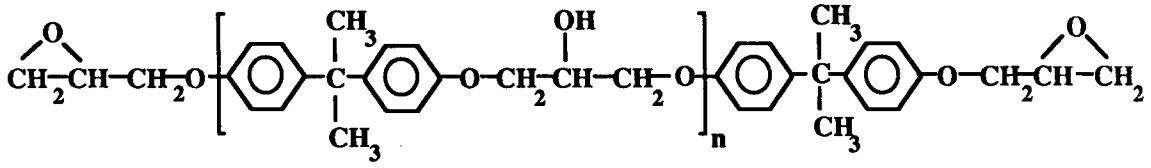

a)

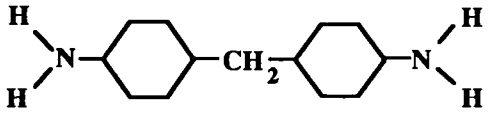

b)

Figure 5 (a) Epoxy EPON 1001F (n = 1.3) and (b) diamine PACM 20 chemical structure.

20, taken in transmission experiments, are presented in Figure 4.

Peaks of interest include peak A at 2960 cm^{-1}, which corresponds to the C—H stretching of the diamine cyclohexane ring, peak B at 1509 cm^{-1}, which corresponds to aromatic C—C stretching of the epoxy, and peak C at 1362 cm^{-1}, characteristic of C—H bending and, therefore, common to both species. The chemical structures of the two compounds are given in Figure 5.

To examine diffusion, spectra were taken in real time and the results for the absorbance of peaks A, B, and C are shown in Figure 6. The decrease in epoxy concentration and the increase in the amine one, as indicated by the respective peak absorptions, provides evidence that the diffusion process takes place in a reasonable time scale. Since band B had the highest absorbance and there were no interferences from neighboring peaks, it was designated as the band to be monitored during the test. The depletion of the epoxy with real time, due to amine diffusion, can be observed by the decrease of the band absorbance in Figure 7.

Analysis for Diffusivity Evaluation

The problem here is treated as a Fickian diffusion problem. The diffusant (amine), of bulk concentration $c_{a\infty}$ at $x = L$ (which is the equilibrium solubility), is penetrating a film of epoxy of thickness L (Fig. 8). By using the no penetration boundary condition at $x = 0$ (due to the crystal surface) and a $c_a = 0$ initial concentration inside the epoxy phase, the

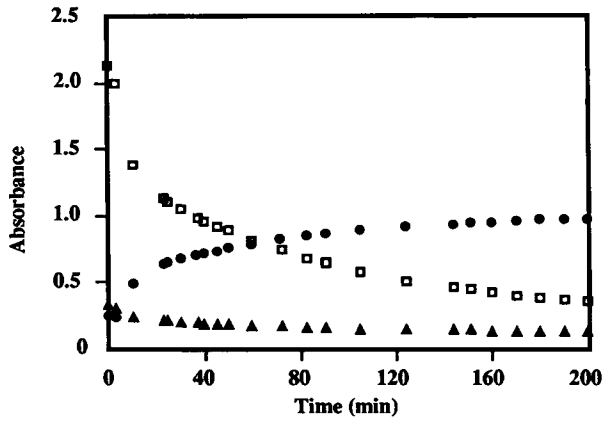

Figure 6 Absorbance vs. time for three characteristic peaks: (● A) 2960 cm^{-1}, (□ B) 1509 cm^{-1}, and (▲ C) 1362 cm^{-1}.

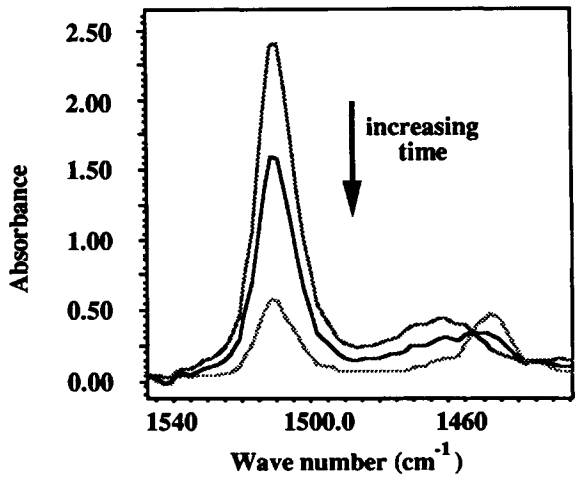

Figure 7 Epoxy characteristic band evolution with time during diffusion experiment.

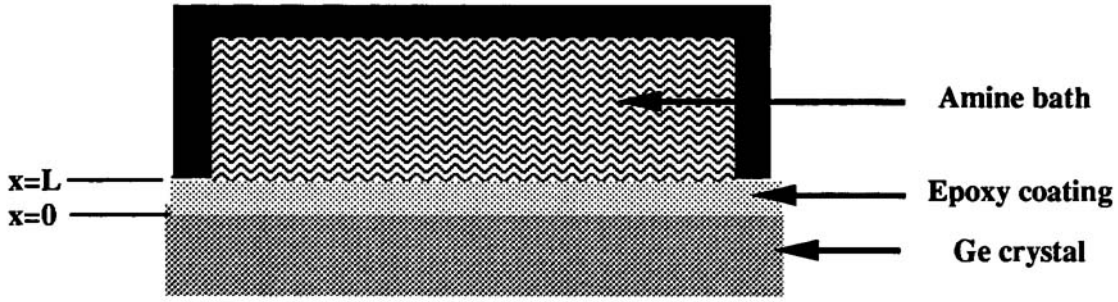

Figure 8 ATR experiment assembly and Cartesian coordinate system for diffusion analysis.

solution to the diffusion equation is given by an infinite sum:

$$c_a(x,t) = c_{a\infty}\left\{1 - \frac{4}{\pi}\sum_{n=0}^{\infty}\frac{(-1)^n}{2n+1}\cos\left(\frac{(2n+1)\pi x}{2L}\right) \times \exp\left(-\left(\frac{(2n+1)\pi}{2L}\right)^2 Dt\right)\right\} \quad (4)$$

where c_a is the concentration of diffusant at any position x in the film at any time t and D is the diffusivity.

The use of Cartesian coordinates in the cylindrical shape surface problem is justified by comparing the thickness of our film, on the order of 10 μm, with the radius of the cylinder, 5 mm. The configuration used in the FTIR-ATR experiment, along with different components, is shown schematically in Figure 8.

Assuming a constant density for the mixture, concentrations for the epoxy component of the mixture can also be evaluated. The epoxy concentration c_e is given by a simple mass balance:

$$c_e(x,t) = c_{e\infty} + c_{a\infty}\frac{4}{\pi}\sum_{n=0}^{\infty}\frac{(-1)^n}{2n+1}\cos\left(\frac{(2n+1)\pi x}{2L}\right) \times \exp\left(-\left(\frac{(2n+1)\pi}{2L}\right)^2 Dt\right) \quad (5)$$

In order to calculate the absorbance of the epoxy band that was monitored during the experiment, a weighted average of the epoxy concentration inside the whole domain is calculated according to eq. (2).

$$A(t) = A_\infty + \frac{32 c_{a\infty} aSL}{\pi} \times \left\{\sum_{n=0}^{\infty}\frac{\frac{(-1)^n}{2n+1}\frac{L}{d_p} + \frac{\pi}{4}\exp\left(-2\frac{L}{d_p}\right)}{((2n+1)\pi)^2 + 16\left(\frac{L}{d_p}\right)^2} \times \exp\left(-\left(\frac{(2n+1)\pi}{2L}\right)^2 Dt\right)\right\}. \quad (6)$$

Performing the appropriate nondimensionalization, for the absorbance of the epoxy band, leads to eq. (7):

$$\frac{A(t) - A_\infty}{A_0 - A_\infty} = \frac{\left\{\sum_{n=0}^{\infty}\frac{\frac{(-1)^n}{2n+1}\frac{L}{d_p} + \frac{\pi}{4}\exp\left(-2\frac{L}{d_p}\right)}{((2n+1)\pi)^2 + 16\left(\frac{L}{d_p}\right)^2} \times \exp\left(-\left(\frac{(2n+1)\pi}{2L}\right)^2 Dt\right)\right\}}{\left\{\sum_{n=0}^{\infty}\frac{\frac{(-1)^n}{2n+1}\frac{L}{d_p} + \frac{\pi}{4}\exp\left(-2\frac{L}{d_p}\right)}{((2n+1)\pi)^2 + 16\left(\frac{L}{d_p}\right)^2}\right\}} \quad (7)$$

where $A(t)$, A_o, and A_∞ are the real time, initial, and equilibrium absorbances, respectively. It is important to note here that there are no optical constants left in eq. (7) and the only parameters in the

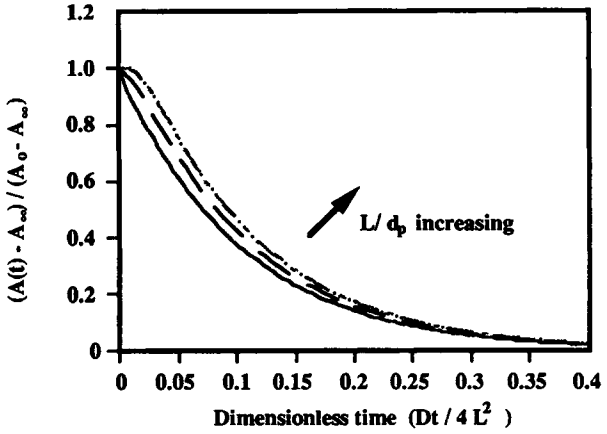

Figure 9 Normalized absorbance vs. dimensionless time. (——) $L/d_p = 1$, (– –) $L/d_p = 2$, (– · – ·) $L/d_p > 5$.

infinite sums are the length scales L and d_p, which can easily be determined. Therefore, only one fitting parameter D is used for the treatment of experimental results. The effect of the ratio L/d_p on the results of the above equation can be seen in Figure 9.

It can be observed that the results are not sensitive to d_p variations for $L/d_p > 5$, which is the case for all our experiments. For those L/d_p values, and keeping in mind that the first terms of the sums are dominant in eq. (7), we have $L/(2n+1)d_p \gg \pi \exp(-2L/d_p)/4$ and, therefore, eq. (7) can be simplified to:

$$\frac{A(t)-A_\infty}{A_o-A_\infty} = \frac{\left\{\sum_{n=0}^{\infty}\left[\frac{(-1)^n}{\pi^2(2n+1)^3+16\left(\frac{L}{d_p}\right)^2(2n+1)}\right] \times \exp\left(-\left(\frac{(2n+1)\pi}{2L}\right)^2 Dt\right)\right\}}{\left\{\sum_{n=0}^{\infty}\left[\frac{(-1)^n}{\pi^2(2n+1)^3+16\left(\frac{L}{d_p}\right)^2(2n+1)}\right]\right\}} \tag{8}$$

Diffusion Experiment Results

Initial experiments were run at room temperature in order to investigate the effects of different length scales. First, an angle of incidence of $\theta = 60°$ was used for the IRE element, leading to a penetration depth of 0.32 μm, according to eq. (1), and using the optical constant for epoxy determined by the

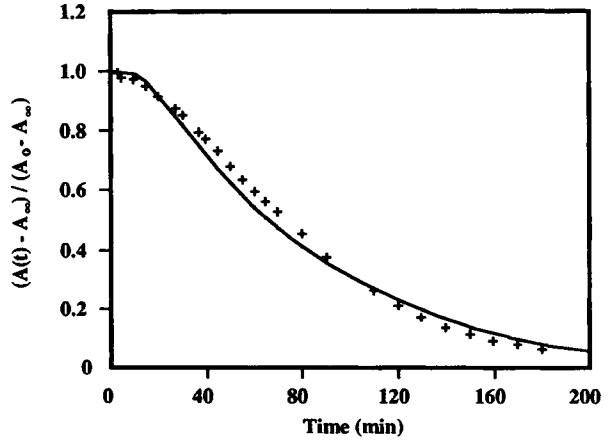

Figure 10 Experimental results for $1/d_p$ ratio of 56: (+) experimental data points and (——) results of fit for Fickian diffusion.

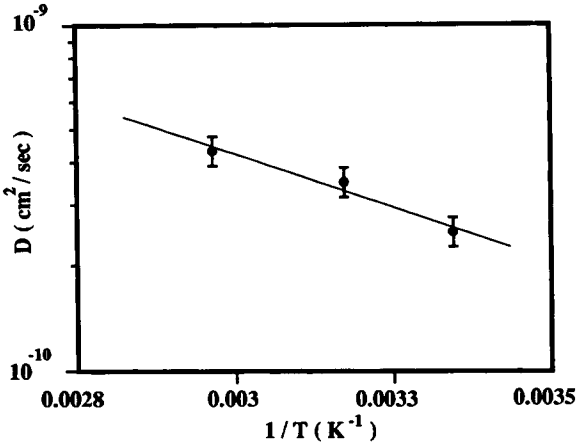

Figure 11 Arrhenius plot for diffusivity of diamine in epoxy layer.

critical angle method. A coating thickness of 18 μm was used for this experimental run, which yielded a ratio of L/d_p equal to 56 with scans being taken only close to the surface. Absorbance results were nondimensionalized according to eq. (7), with A_∞ taken at an experimental time of 1 day, where equilibrium had obviously been achieved. A computer program, using least squares regression, was used to fit experimental results, which gave diffusivity equal to 2.5 10^{-10} cm^2/sec. The interval for D with a 95% significance level was found to be 2.5 $\pm$ 0.2 10^{-10} cm^2/sec. The experimental results, along with the theoretical results for Fickian diffusion, are shown in Figure 10.

A second run was tried, where the coating thickness was kept at the same order of magnitude, 12 μm, but an IRE element of different angle of incidence, $\theta = 30°$, was used. This led to a larger penetration depth of 2 μm and a low ratio L/d_p that was equal to 6. This experiment yielded a similar diffusivity 2.7 $\pm$ 0.5 10^{-10} cm^2/sec, but there was a larger deviation between experimental data and the Fickian curve, especially at small time scales.

Using high L/d_p ratios, experiments were conducted at the temperature range between room temperature and the melting point of the epoxy coating. In particular, 25, 40, and 60°C temperatures were tested. The results of this series of experiments were fitted with an Arrhenius type of equation:

$$D = D_o \exp\left(-\frac{E_o}{RT}\right) \tag{9}$$

The results of the fit are shown in Figure 11, providing us with a D_o that is equal to 4.06 10^{-8} cm^2/sec and an E_o that is equal to 3 kcal/mole.

DISCUSSION

In the above analysis, the penetration depth, d_p, has been assumed to be constant with time and equal to the penetration depth in a film of pure epoxy. This assumption implies a constant refractive index for the material inside the penetration depth boundary, whose composition actually changes with time. This, however, is a reasonable assumption, since eq. (1) shows that penetration depths are not a strong function of the material refractive index. In addition, Figure 9 shows that a small change in d_p should not affect the results if the rest of the assumptions of our anlaysis are valid.

On the other hand, for low L/d_p ratios (lower than 10), higher rates of diffusion were achieved than the ones predicted from our simple Fickian model. This must be attributed to the fact that the interface boundary condition of equilibrium solubility between the two components is not established instantaneously. To be precise, the boundary condition should initially be one of pure amine at the interface. After some time, the interface is formed between the two phases and the results seem to correlate well with theoretical predictions for any L/d_p ratio used.

The use of high L/d_p ratios (higher than 50), such as the one used for the results of Figure 10, showed good correlation between experimental and theoretical data. This could be justified by the fact that the volume of material that is scanned is a small fraction (about $\frac{1}{100}$) of the whole domain and, therefore, interface or boundary condition processes do not interfere with the measurements. Another consideration should be the existence of nonuniformities on the coating thickness. These might lead to two or three dimensional diffusion, but can be neglected if L/d_p ratios are big enough.

Since the epoxy and the amine molecules used in this work can react with each other to form a thermosetting polymer, differential scanning calorimetry studies were done prior to the diffusion experiments. These showed that no reaction takes place at temperatures lower than the melting point of the epoxy, which is 80°C. Therefore, it was safe to assume that the reaction was not a factor at the temperature range of our experimental diffusion studies.

CONCLUSIONS

A spectroscopic technique for the evaluation of diffusivities of small molecules in solid polymers has been described. The FTIR-ATR technique offers the advantages of *in situ* measurements at distances that are close to surfaces over the traditional gravimetric techniques. These characteristics make the method ideal for interfacial work, such as the examination of diffusion and reaction phenomena, taking place near a fiber during the curing of a composite plate.

In this work, the diffusivity of an amine curing agent inside a solid epoxy layer has been investigated over a wide temperature range. Small penetration depths of scanning have been used for the assumption of a one dimensional Fickian diffusion model to be fulfilled. The problem was solved analytically with one fitting parameter, the diffusivity, and good agreement was observed between experimental and theoretical results over a wide range of time. The results of this experimental technique can yield useful information for modelling of the reaction and diffusion processes taking place around a coated or seized fiber during curing. Interfacial properties, and the effects of sizings on them, can be investigated after diffusivities and reaction constants are known.

REFERENCES

1. M. R. Piggott, *Polym. Comp.*, **8**, 291–297 (1987).
2. G. R. Palmese and R. L. McCullough, *J. Appl. Polym. Sci.*, **46**, 1863–1873 (1992).
3. T. P. Skourlis and R. L. McCullough, *Compos. Sci. Techn.*, **49**, 363–368 (1993).
4. J. R. Xu and C. M. Balik, *Appl. Spectrosc.*, **42**(8), 1543–1548 (1988).
5. J. R. Xu and C. M. Balik, *J. Appl. Polym. Sci.*, **38**, 173–183 (1989).
6. T. Nguyen, E. Bird, and D. Bentz, *Quantifying Water at the Organic Film/Hydroxylated Substrate Interface*, Proceedings of the Adhesion Society, February 21–25, 1993, Williamsburg, Virginia, pp. 449–451.
7. J. G. Van Alsten and S. R. Lustig, *Macromolecules*, **25**(19), 5069–5073 (1992).
8. G. T. Fieldson and T. A. Barbari, *Polymer*, **34**(6), 1146–1147 (1993).
9. N. J. Harrick, *Internal Reflection Spectroscopy*, Harrick, Ossining, New York, 1979.

Received August 30, 1993
Accepted October 4, 1993